Behavioural Brain Research 360 (2019) 209–215

Contents lists available at ScienceDirect

Behavioural Brain Research

journal homepage: www.elsevier.com/locate/bbr

Research report

Altered α-amino-3-hydroxy-5-methyl-4-isoxazolepropionic acid (AMPA) receptor function and expression in hippocampus in a rat model of attention-deficit/hyperactivity disorder (ADHD)

Tirill Medin[a,b,c,*], Vidar Jensen[d], Øyvind Skare[e], Jon Storm-Mathisen[c], Øyvind Hvalby[d,1], Linda Hildegard Bergersen[b,c,f]

[a] OsloMet - Oslo Metropolitan University, Faculty of Health Sciences, P.O. Box 4, St. Olavs Plass, 0130, Oslo, Norway
[b] The Brain and Muscle Energy Group, Electron Microscopy Laboratory, Department of Oral Biology, University of Oslo, NO-0316, Oslo, Norway
[c] Synaptic Neurochemistry and Amino Acid Transporters Labs, Division of Anatomy, Department of Molecular Medicine, Institute of Basic Medical Sciences (IMB) and Healthy Brain Ageing Centre (SERTA), University of Oslo, NO-0317, Oslo, Norway
[d] Division of Physiology, Department of Molecular Medicine, Institute of Basic Medical Sciences (IMB), University of Oslo, NO-0317, Oslo, Norway
[e] Department of Occupational Medicine and Epidemiology, National Institute of Occupational Health, Oslo, Norway
[f] Center for Healthy Aging, Department of Neuroscience and Pharmacology, Faculty of Health Sciences, University of Copenhagen, DK-2200, Copenhagen N, Denmark

ARTICLE INFO

Keywords:
Electron microscopy
Hippocampus
Electrophysiology
Field excitatory postsynaptic potentials
Postembedding immunogold quantification
Spontaneously hypertensive rat

ABSTRACT

Glutamatergic α-amino-3-hydroxy-5-methyl-4-isoxazolepropionic acid receptors (AMPARs) carry the bulk of excitatory synaptic transmission. Their modulation plays key roles in synaptic plasticity, which underlies hippocampal learning and memory. A dysfunctional glutamatergic system may negatively affect learning abilities and underlie symptoms of attention-deficit/hyperactivity disorder (ADHD). The aim of this study was to investigate whether the expression and function of AMPARs were altered in ADHD. We recorded AMPAR mediated synaptic transmission at hippocampal excitatory synapses and quantified immunogold labelling density of AMPAR subunits GluA1 and GluA2/3 in a rat model for ADHD; the spontaneously hypertensive rat (SHR). Electrophysiological recordings showed significantly reduced AMPAR mediated synaptic transmission at the CA3-to-CA1 pyramidal cell synapses in stratum radiatum and stratum oriens in SHRs compared to control rats. Electronmicroscopic immunogold quantifications did not show any statistically significant changes in labelling densities of the GluA1 subunit of the AMPAR on dendritic spines in stratum radiatum or in stratum oriens. However, there was a significant increase of the GluA2/3 subunit intracellularly in stratum oriens in SHR compared to control, interpreted as a compensatory effect. The proportion of synapses lacking AMPAR subunit labelling was the same in the two genotypes. In addition, electronmicroscopic examination of tissue morphology showed the density of this type of synapse (i.e., asymmetric synapses on spines), and the average size of the synaptic membranes, to be the same. AMPAR dysfunction, possibly involving molecular changes, in hippocampus may in part reflect altered learning in individuals with ADHD.

1. Introduction

Several studies have focused on monoaminergic neurotransmission in the pathogenesis of attention-deficit/hyperactivity disorder (ADHD) [1], but the glutamatergic system may also be disturbed [2–9]. Glutamate is the main excitatory signaling molecule in the brain and mediates its effect on neighboring neurons by binding to glutamate receptors, especially abundant in the postsynaptic density (PSD) on spines. Glutamatergic α-amino-3-hydroxy-5-methyl-4-isoxazolepropionic acid receptors (AMPARs) are ionotropic receptors that

Abbreviations: ADHD, attention-deficit/hyperactivity disorder; ACSF, artificial cerebrospinal fluid; AMPAR, α-amino-3-hydroxy-5-methyl-4-isoxazolepropionic acid receptor; EPSC, excitatory postsynaptic current; fEPSP, field excitatory postsynaptic potential; GluA1/2R, heterotetramer receptor consisting of AMPAR subunits GluA1 and GluA2; GluA2/3R, receptors consisting of AMPAR subunits GluA2 and GluA3; LTD, long term depression; LTP, long term potentiation; NMDAR, *N*-methyl-D-aspartate receptor; PSD, postsynaptic density; SHR, spontaneously hypertensive rat; SHR/NCrl, SHR from Charles River Germany; WKY, Wistar Kyoto rat; WKY/NHsd, WKY from Harlan Europe UK

* Corresponding author at: OsloMet - Oslo Metropolitan University, Faculty of Health Sciences, P.O. Box 4, St. Olavs Plass, 0130, Oslo, Norway.
E-mail address: tirill.medin@oslomet.no (T. Medin).

[1] Deceased 23th May 2015.

https://doi.org/10.1016/j.bbr.2018.12.028
Received 28 September 2018; Received in revised form 28 November 2018; Accepted 11 December 2018
Available online 12 December 2018

open their ion channel rapidly upon glutamate binding resulting in a fast depolarization of the cell, and carry the bulk of synaptic transmission at excitatory synapses. AMPARs are also involved in long term potentiation (LTP) and long term depression (LTD), which are long term synaptic changes thought to underlie hippocampal learning [10–14]. AMPARs are tetramers comprised of four types of receptor subunits (GluA1-4), and in CA1 hippocampal neurons most AMPARs are heterotetramer receptors consisting of the subunit proteins GluA1 and GluA2 (GluA1/2Rs), or of GluA2 and GluA3 (GluA2/3Rs) [15]. Under basal conditions, GluA1/2Rs contribute up to 80% of the synaptic transmission, while GluA2/3Rs contribute only 20% [16]. GluA2/3 containing AMPARs continuously cycle in and out of synaptic membranes independent of activity [17], whereas the membrane density of GluA1 increases or decreases upon induction of LTP [18] or LTD [19], respectively.

Hyperactivity, impulsivity and inattention are behavioural symptoms of ADHD [20]. Dysfunctional learning is also observed [8,21–23]. Children with ADHD are sensitive to delay in reinforced learning, which may result in impulsivity and inattention. Furthermore, they have problems to extinguish earlier reinforced performance, which may result in an accumulation of reactions seen as hyperactivity [8,24]. The key features characterizing children with ADHD are present in the spontaneously hypertensive rat (SHR), which is validated as the best animal model of ADHD [25,26]. Studies imply that SHR and children with ADHD struggle with reinforcement and extinction in learning processes hypothesized to underlie symptoms of ADHD [8,27–30]. LTP and LTD are commonly referred to as cellular correlates of learning. However, several forms of synaptic plasticity may contribute to learning and memory processes [31], such as changed intrinsic excitability of neurons in hippocampus [32]. Multiple brain regions, including the hippocampus are important in learning and memory [33]. Dysfunctional connection between hippocampus and other brain regions [34] and reduced hippocampal volume in children with ADHD [35] could affect learning processes and further result in ADHD-symptoms [8]. Recent research supports the view that hippocampus dependent learning is altered in children with ADHD [36]. Importantly, hippocampus is a region being explored for the identification of ADHD pathology. Studies from animal models of the disorder suggest abnormalities in neuronal signalling systems within hippocampus [37–40]. However, more studies are needed to further elucidate the potential role of hippocampus in ADHD. Hence, we used SHR as an animal model of ADHD, and its genetic precursor Wistar Kyoto rat (WKY), as control in order to investigate basal synaptic transmission by recording field excitatory postsynaptic potential (fEPSP)s in CA1 stratum radiatum and stratum oriens of the hippocampus as a function of afferent stimulation. We simultaneously investigated excitability of the CA1 pyramidal cells by recording the threshold for generation of the population spikes. GluA1 and GluA2/3 labelling densities were quantified on dendritic spines of CA1 pyramidal cells both in stratum radiatum and stratum oriens by immunogold electron microscopy. Finally, we examined tissue morphology by quantifying synapse density, the proportion of labelled synapses and synapse size.

2. Material and methods

2.1. Animals

The animal experiments were carried out in accordance with procedures and guidelines for animal experiments. Experiments were performed on hippocampal slices from SHR from Charles River, Germany (SHR/NCrl) and WKY from Harlan Europe, UK (WKY/NHsd). SHR/NCrl is the most extensively used, and best evaluated animal model of ADHD [25,26,41], and WKY/NHsd is its optimal control [42]. The rats were sacrificed at p28 (at an age where SHR display an ADHD-like behaviour, but prior to development of hypertension and associated diseases in these models). All rats used in our experiments were male.

2.2. Electrophysiology

The electrophysiological experiments were performed similarly as describes in earlier experiments [4]:

2.2.1. Preparation of hippocampal slices

Experiments were performed on hippocampal slices prepared either from WKY (n = 7) or SHR (n = 8). The animals were killed with inhalation anaesthetic desflurane (Suprane, Baxter), the brains were removed and transverse slices (400 μm) were cut from the middle portion of each hippocampus with a vibroslicer in artificial cerebrospinal fluid (ACSF, 4 °C, bubbled with 95% O_2 - 5% CO_2, pH 7.4) containing (in mM): 124 NaCl, 2 KCl, 1.25 KH_2PO_4, 2 $MgSO_4$, 1 $CaCl_2$, 26 $NaHCO_3$ and 12 glucose. Slices were placed in a humidified interface chamber where the temperature was kept constant at 30 °C and they were perfused with ACSF now containing 2 mM $CaCl_2$.

2.2.2. Stimulation, recording and analysis

Orthodromic synaptic stimuli (< 400 μA, 0.1 Hz) were delivered through a tungsten electrode placed in either stratum radiatum or in stratum oriens. The presynaptic volley and the fEPSP were recorded by a glass electrode (filled with ACSF) placed in the corresponding synaptic layer (stratum radiatum or stratum oriens), while another electrode placed extracellularly in the pyramidal soma layer (stratum pyramidale) monitored the population spike. The afferent fibres in one of the pathways were stimulated at 0.1 Hz with increasing strength (increasing the stimulus duration in steps of 10μs from 0 to 90μs, five consecutive stimulations at each step). To assess synaptic transmission, we measured the amplitude (mV) of the presynaptic volley and the fEPSP (mV) at the different stimulation strengths. The population spike threshold was defined as the appearance of a small negative deflection close to the maximum soma recorded fEPSP positivity. Data were pooled across rats of the same genotype and are presented as mean ± SEM and statistical significance of differences was evaluated using a linear mixed model analysis (SAS 9.2).

2.3. Electron microscopy

2.3.1. Immunogold procedure and analysis

The tissue preparation, immunogold procedure and analysis were performed as in previous experiments [38,43,44] (with the exception of antibody treatment). During the immunogold procedure hippocampal sections from WKY and SHR were incubated with primary antibody rabbit anti-GluA1 (AB 1504, Millipore; 1:100) and rabbit anti GluA2/3 (AB 1506, Millipore; 1:50), and with secondary antibody goat anti-rabbit IgG coupled to 10 nm colloidal gold (British Biocell International, UK; 1:20). We have previously tested the specificity of the primary antibodies [44]. The proportions of labeled synapses, synapse density and synapse size between WKY and SHR were tested for statistical significance using Student's *t*-test.

2.3.2. Immunogold quantification and statistical model

Both membrane associated and intracellular immunogold particles were quantified on the postsynaptic membrane overlying the PSD and up to 100 nm in the intracellular direction in the layer stratum radiatum and statum oriens [43]. The GluA1 immunogold labelling was analyzed in totally 92 + 92 spines from stratum radiatum and 75 + 81 spines from stratum oriens in 4 WKYs and 5 SHRs respectively. The GluA2/3 immunogold labelling was analyzed in totally 86 + 82 spines from stratum radiatum and 52 + 41 spines from stratum oriens in 5 WKYs and 3 SHRs, respectively. Statistical significance of immunolabelling was evaluated using Poisson mixed model [45]. We analyzed the GluA1 and GluA2/3 data separately. We let Y_{ijkl} be immunogold counts for animal *i*, layer *j* (Oriens and Radiatum), region *k* (Intracellular and

Membrane), and repetition *l*. We modeled initially Y_{ijkl} as a Poisson mixed model with log link:

$$Y_{ijk}|u_i,v_{ij},w_{ijk} \sim \text{Poisson}(\lambda_{ijkl}A_{ijkl}) \quad (1)$$

$$\lambda_{ijkl} = e^{\beta g(i),j,k + ui + vij + wijk + \varepsilon ijkl}.$$

Here, A_{ijkl} is the size of the observation area for Y_{ijkl}, and β_{gjk} are fixed effects. The random effects represent variation between animals (u_i), between layers (v_j), between regions (w_{ijk}) The random effects ε_{ijkl} are added to model possible overdispersion, i.e. a greater variability than expected from the Poisson distribution. The term λ_{ijkl} is the intensity of the Poisson distribution and is the expected number of particles in an area of unit size. Models of different complexity were tested by means of likelihood ratio tests. Based on these tests, the model could be simplified by omitting variation between animals, layers and regions. Only, variation inside regions was retained. Our final model was then:

$$Y_{ijk}|u_i,v_{ij},w_{ijk} \sim \text{Poisson}(\lambda_{ijkl}A_{ijkl}) \quad (2)$$

$$\lambda_{ijkl} = e^{\beta g(i),j,k + \varepsilon ijkl}.$$

The fixed effects and variance were estimated by maximum likelihood using Stata function meqrpoisson.

3. Results

3.1. Reduced excitatory synaptic transmission in SHR

In order to assess changes in excitatory synaptic transmission and synaptic excitability we recorded simultaneously either from the apical (stratum radiatum) or from the basal dendritic (stratum oriens) layer, and from the soma layer in the CA1 region of hippocampal slices from SHR (n = 8) and WKY (n = 7). We measured the amplitude of the fiber volley and the fEPSP elicited by different stimulation strengths and, in addition, the corresponding threshold for generation of a population spike.

In SHRs, stratum radiatum evoked fEPSPs (1.3 mV ± 0.1 mV, n = 51 and 2.1 mV ± 0.1 mV, n = 43) for presynaptic fibre volleys of 0.5 and 1.0 mV were severely reduced compared to those elicited in WKYs (1.7 mV ± 0.1 mV, n = 48 and 2.5 mV ± 0.1 mV, n = 36) ($p < 0.05$) (Fig. 1A,C), indicating a reduced synaptic transmission. The excitability tested by synaptic activation was in SHRs, as indicated by threshold for the generation of a population spike (SHR: 1.7 mV ± 0.1 mV, n = 51; WKY: 2.1 mV ± 0.1 mV, n = 48) ($p < 0.05$) (Fig. 1A).

In a similar manner in SHRs, stratum oriens evoked fEPSPs (0.7 mV ± 0.1 mV, n = 39 and 1.2 mV ± 0.1 mV, n = 33) for presynaptic fibre volleys of 0.5 and 1.0 mV showed a significant reduction in size compared to those elicited in WKYs (1.1 mV ± 0.1 mV, n = 35 and 1.7 mV ± 0.1 mV, n = 28) ($p < 0.05$) (Fig. 1B,D), indicating a reduced synaptic transmission. The excitability tested by synaptic activation was unchanged in SHRs (SHR: 1.2 mV ± 0.1 mV, n = 33; WKY: 1.5 mV ± 0.1 mV, n = 33) ($p = 0.25$) (Fig. 1B). At P28, SHRs exhibited a significantly reduced excitatory synaptic transmission (> 25%) both in the radiatum and the oriens pathways, whereas neuronal excitability remained unchanged in the oriens pathway when tested by synaptic activation.

3.2. Electron microscopy

3.2.1. Synapse density, size and labelling

There were no significant changes in synapse density, size or the amount of labelled synapses between WKY and SHR. The density of asymmetric synapses on spines (measured as mean number per μm^2) was quantified by recording the clearly identifiable PSDs in stratum radiatum and stratum oriens in WKY and SHR. The density of synapses in stratum radiatum showed (mean number per μm^2 ± SEM) 0.0598 ± 0.0154 in SHR and 0.0602 ± 0.0079 in WKY ($p = 0.98$); stratum oriens showed 0.0378 ± 0.076 in SHR and 0.0334 ± 0.0069 in WKY ($p = 0.70$). Further, there was no significant difference in the size of the synaptic membrane, as estimated by the length of the PSD profile (mean nm ± SEM): stratum radiatum 220 ± 8, and 211 ± 7 ($p = 0.46$), stratum oriens 214 ± 9 and 227 ± 9 ($p = 0.37$) in SHR and WKY, respectively.

The distribution of immunogold particles was quantified on synapses that had at least one particle over the synaptic membrane and/or the spine cytosol (Fig. 2). Some of the synapses were devoid of immunogold particles, at the postsynaptic membrane as well as overlying the spine cytoplasm. The two genotypes showed no significant differences in the numbers of such non-labelled synapses (mean % of all synapses ± SEM): GluA1 stratum radiatum 60 ± 6 in SHR and 59 ± 5 in WKY ($p = 0.90$), GluA1 stratum oriens 52 ± 3 in SHR and 58 ± 7 in WKY ($p = 0.49$), GluA2/3 stratum radiatum 60 ± 7 in SHR and 70 ± 6 in WKY ($p = 0.90$), GluA2/3 stratum oriens 77 ± 3 in SHR and 68 ± 8 in WKY ($p = 0.33$).

3.2.2. GluA1 and GluA2/3 immunogold labelling analysis and results

The estimated p-values and the confidence intervals of the pairwise differences are given in Tables 1–4.

3.2.2.1. GluA1 quantification. There were no statistically significant changes in GluA1 labelling densities in stratum radiatum or in stratum oriens in SHR compared to WKY ($p > 0.05$). The level of total, membrane and intracellular GluA1 labelling were similar between the two strains in stratum radiatum (Fig. 2A,B) and stratum oriens (Fig. 2C,D), however, there was a tendency towards a decrease in intracellular GluA1 labelling in SHR compared to WKY in stratum oriens ($p = 0.08$). For statistics, see Table 1. There were no significant changes in labelling densities between stratum oriens and stratum radiatum within WKY or SHR (Table 2), although WKY tended to have stronger intracellular labelling in stratum radiatum compared to stratum oriens ($p = 0.071$).

3.2.2.2. GluA2/3 quantification. There was a statistically significant increase in intracellular GluA2/3 labelling level in stratum radiatum in SHR compared to WKY ($p = 0.01$), but no statistically significant differences in total or membrane GluA2/3 labelling levels between WKY and SHR ($p > 0.05$) (Fig. 2E,F). There were no significant differences between WKY and SHR in stratum oriens when we quantified GluA2/3 labelling densities in the different areas (total, membrane and cytoplasm) of dendritic spines ($p > 0.05$) (Fig. 2G,H). See Table 3 for statistics. There was no difference between labelling intensity of GluA2/3 between stratum oriens and stratum radiatum within WKY and SHR (Table 4).

4. Discussion

In the current study, we used SHR/NCrl as an animal model of ADHD, and WKY/NHsd as control. SHR/NCrl is a genetic animal model of ADHD. All SHRs display the core symptoms of ADHD [4,25,26,46–48], including learning disabilities [49,50]. However, it is important to compare SHR/NCrl with its best matched control, the WKY/NHsd [48]. Despite the fact that this rat is the best available model of ADHD-C, the clinical significance of the results must be interpreted with caution, as non-ADHD phenomena could be associated with these rats.

We investigated the threshold for generation of population spikes and the AMPAR mediated synaptic transmission in stratum radiatum and stratum oriens of hippocampus CA1 in the SHR/Ncrl and WKY/NHsd control. We also quantified AMPAR labelling density on dendritic spines of CA1 pyramidal neurons, which are abundant in both stratum oriens and stratum radiatum where they are mainly contacted by

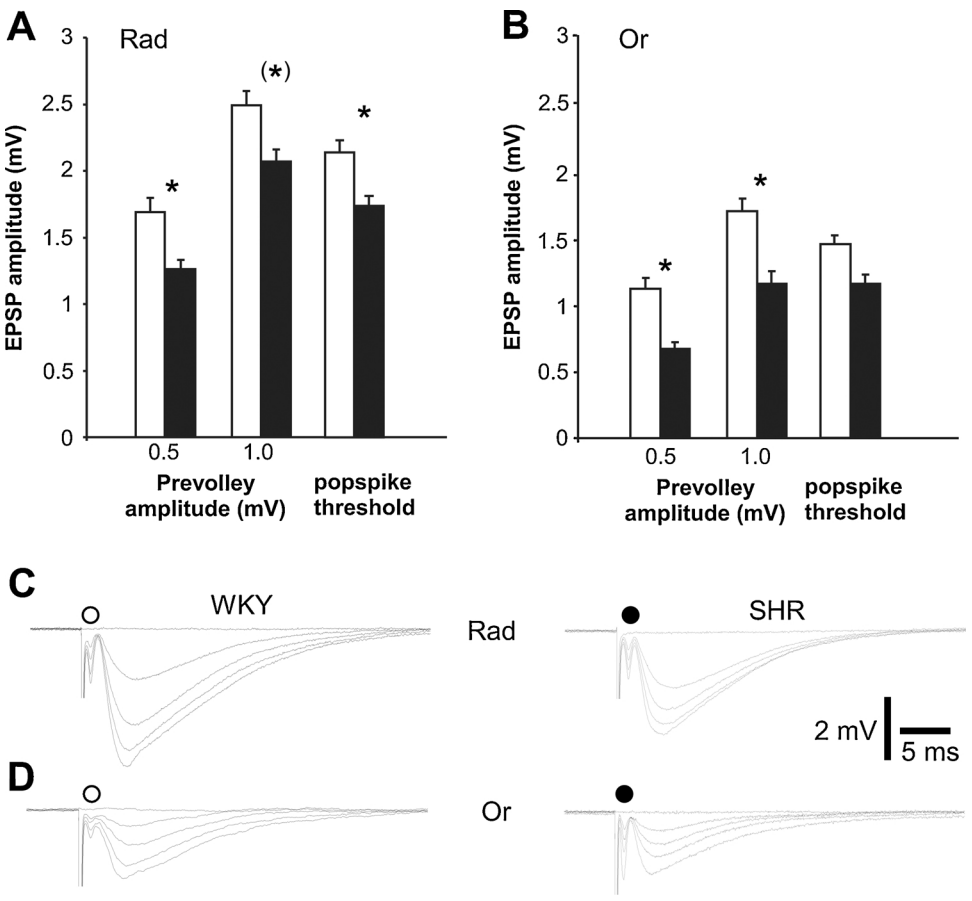

Fig. 1. Reduced glutamatergic transmission in the hippocampal CA3-to-CA1 radiatum and oriens synapses in SHR.
A) fEPSP amplitudes in stratum radiatum (Rad) evoked by prevolleys of 0.5 and 1.0 mV amplitudes in WKY (open columns) and SHR (filled columns). The columns to the right depict the fEPSPs amplitudes necessary to elicit a just detectable population spike in the two genotypes. Data are shown as mean + S.E.M. * indicates $p < 0.05$. (*) indicates $p = 0.05$.
B) As in A, but results are from stratum oriens.
C) Each trace is the mean of five consecutive synaptic responses in stratum radiatum (Rad) evoked by different stimulation strengths in slices from WKY (left) and SHR (right). The prevolleys preceding the fEPSPs are indicated by an open (WKY) or filled circle (SHR).
D) As in C, but the recordings are from stratum oriens.

presynaptic glutamatergic terminals of axons, including the Schaffer collaterals, originating from CA3 pyramidal cells. The electrophysiological recordings demonstrated reduced AMPAR mediated synaptic responses in both stratum oriens and stratum radiatum. These results confirm the results from previous recordings in SHR showing decreased AMPAR mediated synaptic transmission in stratum radiatum [4]. In the current study, the results also extend to be significant in another region of the hippocampus, the stratum oriens. The reduction in synaptic efficacy, represented by the observed 16% to 36% reduction in fEPSP in SHR relative to WKY (our Fig. 1A), corresponds to reductions in fEPSP amplitude previously shown to be associated with significant reductions in learning. For example, a recent paper [51] reported that a 30% reduction of perforant path evoked fEPSP in the dentate gyrus after inhibition of β-adrenoceptors with propranolol (their Fig. 2b) was associated with a dramatic reduction in the acquisition of active avoidance behaviour (their Fig. 2a). Relevant for AMPAR function, behaviour, electrophysiology and microdialysate biochemistry were recorded simultaneously in the same freely moving rats, showing that the changes included a 60% reduction in extracellular glutamate at the recording site (their Fig. 2c).

The reduction in synaptic efficacy recorded in our experiments could not be explained by a reduction in the number or size of the synapses, or by reduced levels of GluA1s or GluA2/3 s, as shown by immunogold quantifications. Furthermore, the amount of labelled synapses was similar between the two strains. The CA3-to-CA1 synapses in hippocampus comprise a population of "silent" synapses lacking AMPAR [52]. The proportion of unlabelled CA3-to-CA1 synapses observed in stratum radiatum of CA1 in the present study (60%–70%) is larger than that observed by Takumi et al. (25%–30%) [52]. This difference is likely caused by the fact that the authors used different sets of antibodies, combined antibodies to GluA1, GluA2/3 and GluA4, and observed each synapse in three consecutive sections, resulting in an increased probability of labelling an AMPAR complex, whereas we used single antibodies on single sections. Importantly, the proportion of synapses with and without AMPAR labelling did not differ between SHR and WKY controls, excluding this as an explanation of the observed difference in AMPAR function.

The reduced synaptic transmission is not verified by low AMPAR labelling density. Importantly, genetic variants or phosphorylation and other posttranslational regulations may change receptor binding site, membrane trafficking, ability to interact with other receptors or kinetics, changes that could impair receptor function without affecting receptor density. Such changes may modify synaptic strength and cellular correlates of learning [53]. Molecular interactions are known to occur between AMPARs and dopamine receptors [54,55]. We previously demonstrated low levels of dopamine D5 receptors [38] as well as a significant N-methyl-D-aspartate receptor (NMDAR) subunit NR2B dependent contribution to LTP in hippocampus in SHR [4]. Dopamine is an important neuromodulator of glutamatergic signalling and may affect both function and delivery of glutamatergic receptors to the synapse trough protein kinase A dependent phosphorylation [56,57]. The reduced transmission observed in SHR could be related to impaired function of GluA1/2Rs, which contribute 80% of the basal synaptic transmission [16]. We found significantly higher labelling density of GluA2/3 intracellularly in SHR. However, consistent with the intracellular location observed, synaptic efficacy was not rescued by the increased level of GluA2/3 in SHR. Even if some of the added GluA2/3Rs get inserted into the membrane, they may not improve function, due to the fact that GluA3Rs have considerably lower conductance and they desensitize three times faster than GluA1Rs [58]. Interestingly, we found the increased density of GluA2/3 intracellularly in SHR up to 100 nm into the spine head. In rat hippocampal neurons, AMPARs are concentrated into a few nanodomains of ~70 nm inside the spine head [59]. PSD-95 is important for the assembly of AMPARs in intracellular

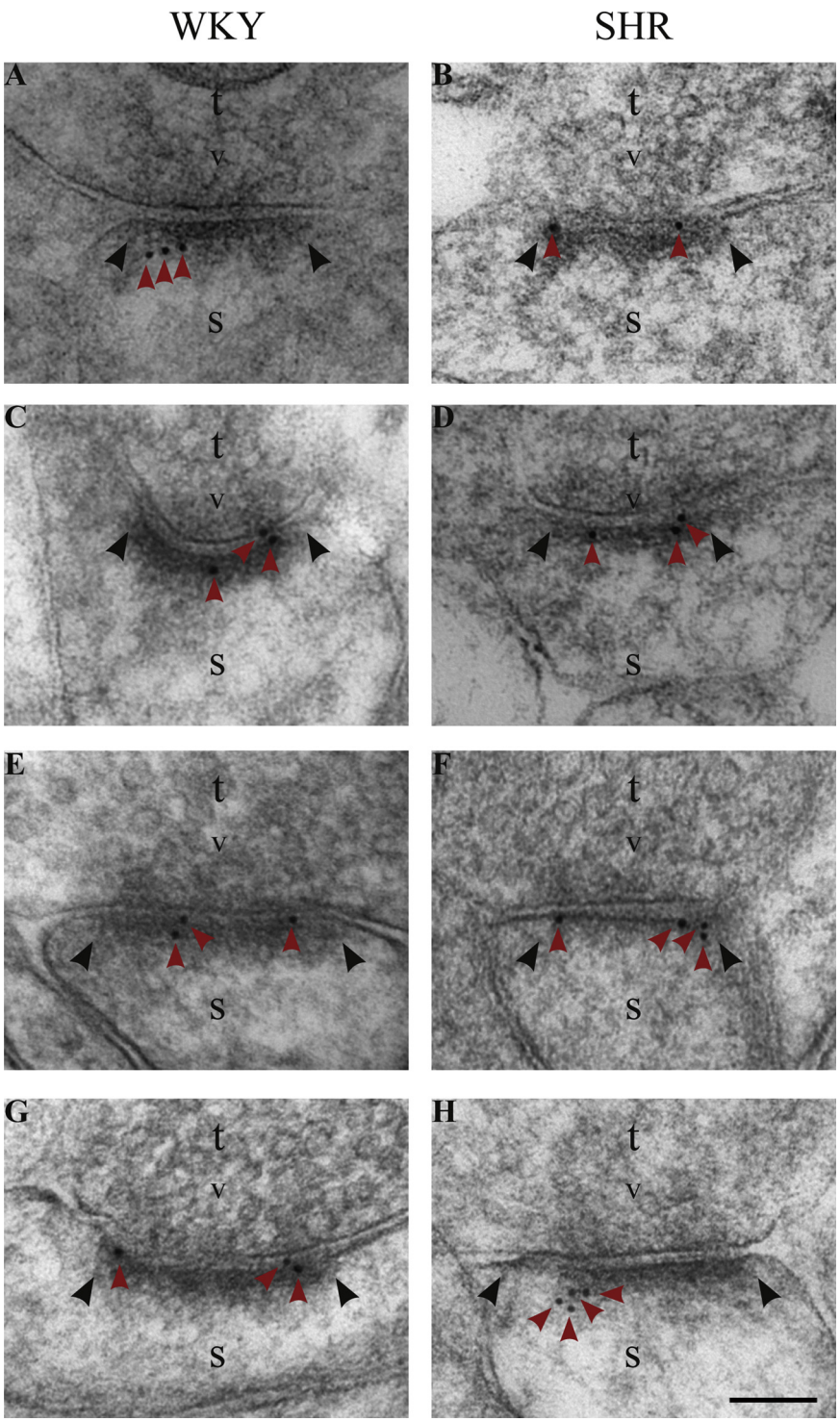

Fig. 2. AMPAR subunit GluA1 and GluA2/3 immunogold labelling.
Electron micrographs showing a glutamatergic terminal (t) with vesicles (v) contacting a postsynaptic dendritic spine (s) in CA1 stratum radiatum and stratum oriens of hippocampus. GluA1 and GluA2/3 subunits of the AMPAR were labelled by immunogold particles (red arrowheads) and quantified along the postsynaptic membrane overlying the PSD (between black arrowheads) and in the cytoplasm of dendritic spines. (Scale bar = 100 nm).The Micrographs from WKY (left) and SHR (right) show immunogold labelling of GluA1 in stratum radiatum (A,B) and stratum oriens (C,D), and GluA2/3 in stratum radiatum (E,F) and stratum oriens (G,H).

Table 1
GluA1: Differences between groups (SHR - WKY). Estimates, p-values and 95% confidence intervals.

Layer	Region	Estimate	P-value	Lower	Upper
Oriens	Intracellular	−0.081	0.739	−0.559	0.396
Oriens	Membrane	−0.202	0.206	−0.111	0.515
Radiatum	Intracellular	−0.360	0.077	−0.759	0.039
Radiatum	Membrane	−0.030	0.839	−0.329	0.267
Oriens	Total	0.134	0.245	−0.081	0.359
Radiatum	Total	−0.122	0.250	−0.331	0.086

Table 2
GluA1: Differences between layers (radiatum - oriens). Estimates, p-values and 95% confidence intervals.

Group	Region	Estimate	P-value	Lower	Upper
WKY	Intracellular	0.389	0.071	−0.033	0.811
WKY	Membrane	0.018	0.911	−0.293	0.329
SHR	Intracellular	0.110	0.637	−0.347	0.567
SHR	Membrane	−0.215	0.160	−0.515	0.085
WKY	Total	0.119	0.284	−0.099	0.336
SHR	Total	−0.137	0.215	−0.353	0.079

Table 3
GluA2/3: Differences between groups (SHR - WKY). Estimates, p-values and 95% confidence intervals.

Layers	Region	Estimate	P-value	Lower	Upper
Oriens	Intracellular	0.044	0.883	−0.544	0.632
Oriens	Membrane	0.227	0.296	−0.198	0.653
Radiatum	Intracellular	0.574	0.010	0.136	1.011
Radiatum	Membrane	−0.197	0.228	−0.518	0.123
Oriens	Total	0.179	0.264	−0.135	0.492
Radiatum	Total	0.033	0.786	−0.203	0.268

Table 4
GluA2/3: Differences between layers (Radiatum - Oriens). Estimates, p-values and 95% confidence intervals.

Group	Region	Estimate	P-value	Lower	Upper
WKY	Intracellular	−0.249	0.344	−0.763	0.266
WKY	Membrane	0.180	0.332	−0.184	0.543
SHR	Intracellular	0.281	0.292	−0.241	0.803
SHR	Membrane	−0.244	0.219	−0.634	0.145
WKY	Total	0.052	0.706	−0.218	0.322
SHR	Total	−0.094	0.516	−0.378	0.190

nanodomains: Overexpression of PSD95 is followed by an accumulation of AMPAR in intracellular domains and increased miniature excitatory postsynaptic current (EPSC) amplitude [60], whereas reduced expression of PSD-95 leads to decreased numbers of AMPARs per domain and reduced miniature EPSC amplitude [59,61]. The function of intracellular AMPAR clusters is currently not fully understood but they possibly affect synaptic transmission by modifying intracellular cluster size, position, or receptor content with no changes in total receptor number [61,62]. The various pools of AMPARs and their dynamic may have impacts on several forms of synaptic plasticity and learning, and may be important therapeutic goals in the future treatment of brain disorders [62–64].

The last decades, glutamate receptors have been the target for novel drug development to treat neurological disorders [65]. As summarized by Froestl et al. (2014), agents acting on different types of glutamate receptors may be useful to treat ADHD [65]. AMPAR modulators enhance cognitive performance [66] and reduce hyperactivity in rats [67] and show promising results in children with ADHD [67]. However, glutamate receptors are ubiquitously expressed in the brain and pharmacological manipulation of AMPARs may have a broad impact on CNS function and behaviour. Consequently, intracellular protein complexes controlling the assembly of AMPARs into different subcellular domains are currently emerging as more specific therapeutic goals in the treatment of neurodevelopmental disorders [68,69], as these proteins are more heterogeneously expressed in the brain, as compared to AMPARs. Hence, it would be interesting to further study potential mechanisms underlying the abnormal assembly of AMPAR into different pools in SHR, as observed in our study.

The lack of specific antibodies for each of the specific GluA1-3 subunits is a methodological concern. The GluA1 antibody used in our study recognizes the c-terminus of the GluA1 peptide sequence. In CA1 pyramidal cells, GluA1/2 heteromers dominate (only 8% are GluA1 homomers) [15], therefore, the GluA1 labelling densities quantified in our study mainly reflect GluA1/2 heteromers. The GluA2/3 antibody used in this study, detects amino acid sequences in the c-terminal of both GluA2 and GluA3, and will consequently label both GluA1/2Rs and GluA2/3Rs, which are present in nearly equal proportions in CA1 hippocampus [15]. Nevertheless, the GluA2/3 antibody probably mainly binds GluA2/3Rs as these receptors have twice as many potential antibody binding sites compared to GluA1/2Rs. A previous genetic study has shown increased GluA2 mRNA, but decreased GluA3 mRNA in SHR compared to WKY [70]. However, we were not able to distinguish between these two subunits in this study.

Low AMPAR mediated transmission accompanied by low expression of surface GluA1 and GluA2 AMPAR subunits has previously been observed in prefrontal cortex in SHR [71]. However, total amount of GluA1 and GluA2 levels was similar between WKY and SHR, as observed in our study. Interestingly, methylphenidate a frequently used treatment in ADHD, normalizes synaptic transmission in prefrontal cortex in SHR. Methylphenidate may enhance diffusion, and incorporation of AMPAR at hippocampal CA3-CA1 synapses [72]. Under basal conditions, GluA1/2 and GluA2/3 heteromers are present in the postsynaptic membrane of dendritic spines. Additional receptors may be recruited to the postsynaptic membrane overlying the PSD by lateral diffusion from extrasynaptic sites or by direct exocytosis of receptors present in vesicular organelles in the cytoplasm of the spine. The areas we investigated were limited to the postsynaptic membrane overlying the PSD, and the area directly below the PSD inside the spine. Hence, it is possible that there exist changes in receptor level that was not identified in this study. In conclusion, our results suggest alterations in glutamate signaling in hippocampus in SHR, which could disturb processes of learning in ADHD.

Conflict of interest

There is no conflict of interest.

Funding

This work was supported by the Molecular Life Science, University of Oslo, and the Research Council of Norway.

Declaration of interest

None.

Acknowledgements

We would like to acknowledge Terje Sagvolden (deceased 12 January 2011) for validating the SHR/NCrl used as an animal model of ADHD and WKY/NHsd used as control [26].

References

[1] C. Scassellati, et al., Biomarkers and attention-deficit/hyperactivity disorder: a systematic review and meta-analyses, J Am. Acad. Child Adolesc. Psychiatry 51 (10) (2012) 1003–1019.
[2] J. Adams, et al., Glutamate receptor, ionotropic, N-methyl D-aspartate 2A (GRIN2A) gene as a positional candidate for attention-deficit/hyperactivity disorder in the 16p13 region, Mol. Psychiatry 9 (5) (2004) 494–499.
[3] M.P. Carey, et al., Differential distribution, affinity and plasticity of dopamine D-1 and D-2 receptors in the target sites of the mesolimbic system in an animal model of ADHD, Behav. Brain Res 94 (1) (1998) 173–185.
[4] V. Jensen, et al., N-methyl-D-aspartate receptor subunit dysfunction at hippocampal glutamatergic synapses in an animal model of attention-deficit/hyperactivity disorder, Neuroscience 158 (1) (2009) 353–364.
[5] M. Lehohla, L. Kellaway, V.A. Russell, NMDA receptor function in the prefrontal cortex of a rat model for attention-deficit hyperactivity disorder, Metab. Brain Dis. 19 (1-2) (2004) 35–42.
[6] F.P. MacMaster, et al., Proton spectroscopy in medication-free pediatric attention-deficit/hyperactivity disorder, Biol. Psychiatry 53 (2) (2003) 184–187.
[7] E. Perlov, et al., Reduced cingulate glutamate/glutamine-to-creatine ratios in adult patients with attention deficit/hyperactivity disorder – a magnet resonance spectroscopy study, J Psychiatr. Res 41 (11) (2007) 934–941.
[8] T. Sagvolden, et al., A dynamic developmental theory of attention-deficit/hyperactivity disorder (ADHD) predominantly hyperactive/impulsive and combined subtypes, Behav. Brain Sci. 28 (3) (2005) 397–419.
[9] D. Turic, et al., Follow-up of genetic linkage findings on chromosome 16p13: evidence of association of N-methyl-D aspartate glutamate receptor 2A gene polymorphism with ADHD, Mol. Psychiatry 9 (2) (2004) 169–173.
[10] G.L. Collingridge, J.T. Isaac, Y.T. Wang, Receptor trafficking and synaptic plasticity, Nat. Rev. Neurosci. 5 (12) (2004) 952–962.
[11] R.C. Malenka, M.F. Bear, LTP and LTD: an embarrassment of riches, Neuron 44 (1) (2004) 5–21.
[12] R.C. Malenka, R.A. Nicoll, Long-term potentiation–a decade of progress? Science

285 (5435) (1999) 1870–1874.
[13] D.J. Sanderson, et al., The role of the GluR-a (GluR1) AMPA receptor subunit in learning and memory, Prog. Brain Res. 169 (2008) 159–178.
[14] J.R. Whitlock, et al., Learning induces long-term potentiation in the hippocampus, Science 313 (5790) (2006) 1093–1097.
[15] R.J. Wenthold, et al., Evidence for multiple AMPA receptor complexes in hippocampal CA1/CA2 neurons, J. Neurosci. 16 (6) (1996) 1982–1989.
[16] W. Lu, et al., Subunit composition of synaptic AMPA receptors revealed by a single-cell genetic approach, Neuron 62 (2) (2009) 254–268.
[17] S.G. McCormack, R.L. Stornetta, J.J. Zhu, Synaptic AMPA receptor exchange maintains bidirectional plasticity, Neuron 50 (1) (2006) 75–88.
[18] M. Park, et al., Recycling endosomes supply AMPA receptors for LTP, Science 305 (5692) (2004) 1972–1975.
[19] R.C. Carroll, et al., Rapid redistribution of glutamate receptors contributes to long-term depression in hippocampal cultures, Nat. Neurosci. 2 (5) (1999) 454–460.
[20] American Psychiatric Association, Diagnostic and Statistical Manul of Mental. Disorders, 5th ed., American Psychiatric Publishing, Washington, DC, 2013.
[21] V.I. Douglas, P.A. Parry, Effects of reward on delayed reaction time task performance of hyperactive children, J. Abnorm. Child Psychol. 11 (2) (1983) 313–326.
[22] T. Sagvolden, J.A. Sergeant, Attention deficit/hyperactivity disorder–from brain dysfunctions to behaviour, Behav. Brain Res. 94 (1) (1998) 1–10.
[23] E.J. Sonuga-Barke, E. Taylor, The effect of delay on hyperactive and non-hyperactive children's response times: a research note, J. Child Psychol. Psychiatry 33 (6) (1992) 1091–1096.
[24] T. Sagvolden, et al., Altered reinforcement mechanisms in attention-deficit/hyperactivity disorder, Behav. Brain Res. 94 (1) (1998) 61–71.
[25] V.A. Russell, Overview of animal models of attention deficit hyperactivity disorder (ADHD), Curr. Protoc. Neurosci (2011) Chapter 9: p. Unit9.
[26] T. Sagvolden, E.B. Johansen, Rat models of ADHD, Curr. Top. Behav. Neurosci. 9 (2012) 301–315.
[27] H. Aase, T. Sagvolden, Infrequent, but not frequent, reinforcers produce more variable responding and deficient sustained attention in young children with attention-deficit/hyperactivity disorder (ADHD), J. Child Psychol. Psychiatry 47 (5) (2006) 457–471.
[28] H. Aase, A. Meyer, T. Sagvolden, Moment-to-moment dynamics of ADHD behaviour in South African children, Behav. Brain Funct. 2 (2006) 11.
[29] H. Aase, T. Sagvolden, Moment-to-moment dynamics of ADHD behaviour, Behav. Brain Funct. 1 (2005) 12.
[30] E.B. Johansen, et al., Attention-deficit/hyperactivity disorder (ADHD) behaviour explained by dysfunctioning reinforcement and extinction processes, Behav. Brain Res. 130 (1-2) (2002) 37–45.
[31] M. Di Filippo, et al., Short-term and long-term plasticity at corticostriatal synapses: implications for learning and memory, Behav. Brain Res. 199 (1) (2009) 108–118.
[32] W. Zhang, D.J. Linden, The other side of the engram: experience-driven changes in neuronal intrinsic excitability, Nat. Rev. Neurosci. 4 (11) (2003) 885–900.
[33] J. Goodman, et al., Annual research review: the neurobehavioral development of multiple memory systems–implications for childhood and adolescent psychiatric disorders, J. Child Psychol. Psychiatry 55 (6) (2014) 582–610.
[34] J. Posner, et al., A multimodal MRI study of the hippocampus in medication-naive children with ADHD: what connects ADHD and depression? Psychiatry Res. 224 (2) (2014) 112–118.
[35] M. Hoogman, et al., Subcortical brain volume differences in participants with attention deficit hyperactivity disorder in children and adults: a cross-sectional mega-analysis, Lancet Psychiatry 4 (4) (2017) 310–319.
[36] P. Robaey, et al., Stop and look! Evidence for a bias towards virtual navigation response strategies in children with ADHD symptoms, Behav. Brain Res. 298 (Pt A) (2016) 48–54.
[37] V. Jensen, et al., N-methyl-D-aspartate receptor subunit dysfunction at hippocampal glutamatergic synapses in an animal model of attention-deficit/hyperactivity disorder, Neuroscience 158 (1) (2009) 353–364.
[38] T. Medin, et al., Low dopamine D5 receptor density in hippocampus in an animal model of attention-deficit/hyperactivity disorder (ADHD), Neuroscience 242 (2013) 11–20.
[39] T.L. Sterley, F.M. Howells, V.A. Russell, Nicotine-stimulated release of [3H]norepinephrine is reduced in the hippocampus of an animal model of attention-deficit/hyperactivity disorder, the spontaneously hypertensive rat, Brain Res. 1572 (2014) 1–10.
[40] T.L. Sterley, F.M. Howells, V.A. Russell, Evidence for reduced tonic levels of GABA in the hippocampus of an animal model of ADHD, the spontaneously hypertensive rat, Brain Res. 1541 (2013) 52–60.
[41] T. Sagvolden, Behavioral validation of the spontaneously hypertensive rat (SHR) as an animal model of attention-deficit/hyperactivity disorder (AD/HD), Neurosci. Biobehav. Rev 24 (1) (2000) 31–39.
[42] T. Sagvolden, et al., The spontaneously hypertensive rat model of ADHD–the importance of selecting the appropriate reference strain, Neuropharmacology 57 (7-8) (2009) 619–626.
[43] T. Medin, et al., Dopamine D5 receptors are localized at asymmetric synapses in the rat hippocampus, Neuroscience 192 (2011) 164–171.
[44] C.E. Regnell, et al., Hippocampal adult neurogenesis is maintained by Neil3-dependent repair of oxidative DNA lesions in neural progenitor cells, Cell Rep 2 (3) (2012) 503–510.
[45] StataCorp, Stata Statistical Software: Release 13. College Station, TX: StataCorp LP, (2013).
[46] K.S. Dervola, et al., Marine omega-3 polyunsaturated fatty acids induce sex-specific changes in reinforcer-controlled behaviour and neurotransmitter metabolism in a spontaneously hypertensive rat model of ADHD, Behav. Brain Funct. 8 (1) (2012) 56.
[47] T. Sagvolden, et al., Behavioral and genetic evidence for a novel animal model of attention-deficit/hyperactivity disorder predominantly inattentive subtype, Behav. Brain Funct. 4 (2008) 56.
[48] T. Sagvolden, et al., The spontaneously hypertensive rat model of ADHD–the importance of selecting the appropriate reference strain, Neuropharmacology 57 (7-8) (2009) 619–626.
[49] E.B. Johansen, P.R. Killeen, T. Sagvolden, Behavioral variability, elimination of responses, and delay-of-reinforcement gradients in SHR and WKY rats, Behav. Brain Funct. 3 (2007) 60.
[50] E.B. Johansen, T. Sagvolden, G. Kvande, Effects of delayed reinforcers on the behavior of an animal model of attention-deficit/hyperactivity disorder (ADHD), Behav. Brain Res. 162 (1) (2005) 47–61.
[51] J. Lv, et al., Activation of beta-adrenoceptor facilitates active avoidance learning through enhancement of glutamate levels in the hippocampal dentate gyrus, Neuroreport 28 (15) (2017) 973–979.
[52] Y. Takumi, et al., Different modes of expression of AMPA and NMDA receptors in hippocampal synapses, Nat. Neurosci. 2 (7) (1999) 618–624.
[53] T.E. Chater, Y. Goda, The role of AMPA receptors in postsynaptic mechanisms of synaptic plasticity, Front. Cell. Neurosci. 8 (2014) 401.
[54] S.Z. Chao, et al., D(1) dopamine receptor stimulation increases GluR1 phosphorylation in postnatal nucleus accumbens cultures, J. Neurochem. 81 (5) (2002) 984–992.
[55] G.L. Snyder, et al., Regulation of phosphorylation of the GluR1 AMPA receptor in the neostriatum by dopamine and psychostimulants in vivo, J. Neurosci. 20 (12) (2000) 4480–4488.
[56] T.G. Banke, et al., Control of GluR1 AMPA receptor function by cAMP-dependent protein kinase, J. Neurosci. 20 (1) (2000) 89–102.
[57] D.B. Scott, T.A. Blanpied, M.D. Ehlers, Coordinated PKA and PKC phosphorylation suppresses RXR-mediated ER retention and regulates the surface delivery of NMDA receptors, Neuropharmacology 45 (6) (2003) 755–767.
[58] T.G. Banke, et al., Identification of amino acid residues in GluR1 responsible for ligand binding and desensitization, J. Neurosci. 21 (9) (2001) 3052–3062.
[59] D. Nair, et al., Super-resolution imaging reveals that AMPA receptors inside synapses are dynamically organized in nanodomains regulated by PSD95, J. Neurosci. 33 (32) (2013) 13204–13224.
[60] C. Bats, L. Groc, D. Choquet, The interaction between stargazin and PSD-95 regulates AMPA receptor surface trafficking, Neuron 53 (5) (2007) 719–734.
[61] H.D. MacGillavry, et al., Nanoscale scaffolding domains within the postsynaptic density concentrate synaptic AMPA receptors, Neuron 78 (4) (2013) 615–622.
[62] E. Moretto, M. Passafaro, Recent findings on AMPA receptor recycling, Front. Cell. Neurosci. 12 (2018) p. 286.
[63] D. Choquet, Linking nanoscale dynamics of AMPA receptor organization to plasticity of excitatory synapses and learning, J. Neurosci. 38 (44) (2018) 9318–9329.
[64] R.L. Huganir, R.A. Nicoll, AMPARs and synaptic plasticity: the last 25 years, Neuron 80 (3) (2013) 704–717.
[65] W. Froestl, A. Muhs, A. Pfeifer, Cognitive enhancers (nootropics). Part 1: drugs interacting with receptors. Update 2014, J. Alzheimers Dis. 41 (4) (2014) 961–1019.
[66] E. Hamlyn, et al., The ampakine, Org 26576, bolsters early spatial reference learning and retrieval in the morris water maze: a subchronic, dose-ranging study in rats, Behav. Pharmacol. 20 (7) (2009) 662–667.
[67] L.A. Adler, et al., A translational approach to evaluate the efficacy and safety of the novel AMPA receptor positive allosteric modulator org 26576 in adult attention-deficit/hyperactivity disorder, Biol. Psychiatry 72 (11) (2012) 971–977.
[68] E. Moretto, et al., Glutamatergic synapses in neurodevelopmental disorders, Prog. Neuropsychopharmacol. Biol. Psychiatry 84 (Pt B) (2018) 328–342.
[69] K. Lee, et al., AMPA receptors as therapeutic targets for neurological disorders, Adv. Protein Chem. Struct. Biol. 103 (2016) 203–261.
[70] T. Dasbanerjee, et al., A comparison of molecular alterations in environmental and genetic rat models of ADHD: a pilot study, Am. J Med. Genet. B Neuropsychiatr. Genet 147B (8) (2008) 1554–1563.
[71] J. Cheng, et al., Disrupted glutamatergic transmission in prefrontal cortex contributes to behavioral abnormality in an animal model of ADHD, Neuropsychopharmacology 42 (10) (2017) 2096–2104.
[72] C. Rozas, et al., Methylphenidate amplifies long-term potentiation in rat hippocampus CA1 area involving the insertion of AMPA receptors by activation of beta-adrenergic and D1/D5 receptors, Neuropharmacology 99 (2015) p. 15-27.